Transition metal complexes with sulfur ligands
Part LXXIX*. Crown thioether complexes of iron, cobalt, nickel and copper with bzo_2-18S6. X-ray structure analysis of $[Ni(bzo_2\text{-}18S6)][B(C_6H_5)_4]_2$ (bzo_2-18S6 = 2,3,11,12-dibenzo-1,4,7,10,13,16-hexathiacyclooctadeca-2,11-diene)

Dieter Sellmann**, Hans-Peter Neuner and Falk Knoch
Institut für Anorganische Chemie der Universität Erlangen-Nürnberg, Egerlandstrasse 1, W-8520 Erlangen (FRG)

(Received May 24, 1991)

Abstract

Reaction of bzo_2-18S6 (2,3,11,12-dibenzo-1,4,7,10,13,16-hexathiacyclooctadeca-2,11-diene) with Fe, Co, Ni and Cu salts yields the corresponding metal complexes $[M(bzo_2\text{-}18S6)]^{n+}$. Their trifluoromethanesulfonate salts were characterized by spectroscopic and electrochemical methods and the structure of $[Ni(bzo_2\text{-}18S6)][B(C_6H_5)_4]_2$ was elucidated by X-ray structure determination. It crystallizes in space group $P2_1/n$ with $a = 1497.8(4)$, $b = 1096.5(4)$, $c = 1772.5(5)$ pm, $\beta = 104.26(2)°$, $Z = 2$ and $D_{calc} = 1.36$ g/cm^3; $R = 0.061$, $R_w = 0.041$. The nickel centre is surrounded by the six sulfur atoms of the ligand in a slightly distorted octahedron. The Ni–S distances indicate a ligand compression effect of bzo_2-18S6. The different electrochemical behaviour of the $[M(bzo_2\text{-}18S6)]^{n+}$ complexes is discussed.

Introduction

Recently we reported the high yield synthesis of bzo_2-18S6 via template alkylation [2]. bzo_2-18S6 (2,3,11,12-dibenzo-1,4,7,10,13,16-hexathiacyclooctadeca-2,11-diene) is the sulfur analogue of dibenzo-18-crown-6 [3].

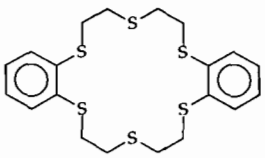

bzo_2-18S6 ≈ L

Whereas crown ethers readily coordinate to 'hard' ions, e.g. alkali metal ions, the sulfur donors are expected to make crown thioethers suitable ligands for 'soft' transition metal ions in low oxidation states. This expectation has been verified in the syntheses of numerous crown thioether complexes. They allowed the investigation of special properties impressed on metal centres by thioethers, e.g. unusual redox behaviour and electron spectra. Crown thioether complexes are also important with respect to the active centres of numerous metal redox enzymes containing sulfur coordinated transition metals [4], and with regard to the development of radio diagnosticals and pharmaceuticals, because many of them show surprising complex stability. These results were comprehensively reviewed recently [5, 6].

Very often crown thioethers do not exhibit a preorganization favourable for coordination as found with oxygen crown ethers. This holds also for bzo_2-18S6 that exhibits a nearly planar array of six S donors in the free state [2]. It disfavours the coordination of bzo_2-18S6 to metal centres in (pseudo)octahedral complexes, but as the high tendency of formation of $[Ru(bzo_2\text{-}18S6)]^{2+}$ is showing [7], this disadvantage can be compensated and overcome if strong metal thioether bonds are formed. For these reasons we considered it worthwhile to investigate the coordination of bzo_2-18S6 to 3d metals and want to report here the results on Fe, Co, Ni and Cu.

Experimental

General

All operations were carried out under nitrogen, Schlenk techniques being used. Solvents were dried

*For part LXXVIII see ref. 1.
**Author to whom correspondence should be addressed.

0020-1693/91/$3.50

TABLE 1. Summary of crystallographic data and data collection procedures of $[Ni(bzo_2\text{-}18S6)][B(C_6H_5)_4]_2$

Formula	$[Ni(bzo_2\text{-}18S6)][B(C_6H_5)_4]_2$ $B_2C_{68}H_{64}NiS_6$
Mr	1153.98
Space group	$P2_1/n$
Crystal system	monoclinic
Cell dimensions	
a (pm)	1497.8(4)
b (pm)	1096.5(4)
c (pm)	1772.5(5)
β (°)	104.26(2)
Molecules/unit cell	2
Cell volume (pm^3)	$2821(2)\times10^6$
D_{calc} (g/cm^3)	1.36
Diffractometer	Nicolet R3m/V
Radiation	Mo Kα
Scan technique	ω-scan
Scan speed (°/min)	3–15
$2\theta_{max}$ (°)	54
Reflections collected	6872
Independent reflections	3988
σ-Criterion	$F>4\sigma$
Observed reflections	2509
Program	SHELXTL-PLUS
Parameters refined	350
R; R_w	0.061; 0.041
Temperature of measurement (K)	200

and distilled before use. Spectra were recorded on the following spectrometers: IR: Zeiss IMR 16 IR; NMR: Jeol JNM-GX 270; UV–Vis: Shimadzu UV-3101 PC; mass spectra: Varian MAT 212 (EI and FD mode). Cyclovoltammograms were run on a PAR 264 A with ROTEL A equipped with a glassy carbon working electrode, Ag/AgCl reference electrode and platinum counter electrode. Redox potentials were referred to NHE via ferrocene as internal standard.

Starting materials were purchased from Aldrich, Fluka and Merck. bzo_2-18S6 [2], $[Co(C_5H_7O_2)_3]$ [8] and $[Ni(C_5H_7O_2)_2]_3$ [9] were prepared by literature methods.

X-ray structure determination of $[Ni(bzo_2\text{-}18S6)][B(C_6H_5)_4]_2$

Single crystals (*c.* $0.4\times0.2\times0.1$ mm) were obtained from a nitroethane solution of $[Ni(bzo_2\text{-}18S6)](CF_3SO_3)_2\cdot C_4H_8O_2$ which was layered with a solution of $Na[B(C_6H_5)_4]$ in n-BuOH. A suitable crystal was sealed in a glass capillary under N_2. The structure was solved by direct methods. Non-hydrogen atoms were refined anisotropically, the aromatic hydrogen atoms were placed at calculated positions and refined as rigid groups, and the H atoms of the methylene groups were placed in ideal tetrahedral positions and rotated around their central carbon atom during refinement. Table 1 contains selected crystallographic data and Table 2 gives the final atomic coordinates.

TABLE 2. Atomic coordinates ($\times10^4$) and equivalent isotropic thermal parameters ($pm^2\times10^{-1}$) of $[Ni(bzo_2\text{-}18S6)][B(C_6H_5)_4]_2$

	x	*y*	*z*	U_{eq}[a]
Ni(1)	0	0	0	16(1)
S(1)	−805(1)	−1823(1)	167(1)	20(1)
S(2)	821(1)	−128(2)	1327(1)	22(1)
S(3)	1241(1)	−1125(1)	−348(1)	21(1)
C(1)	−75(4)	−2415(5)	1061(3)	25(3)
C(2)	295(4)	−1435(5)	1671(3)	25(2)
C(3)	1938(4)	−664(5)	1240(3)	27(3)
C(4)	1925(4)	−1585(6)	599(3)	27(2)
C(15)	−1758(4)	−1281(6)	516(3)	19(2)
C(14)	−2331(4)	−2143(7)	724(3)	32(3)
C(13)	−3069(5)	−1755(7)	1004(4)	38(3)
C(12)	−3236(5)	−540(7)	1091(4)	46(4)
C(11)	−2664(4)	324(6)	886(3)	34(3)
C(10)	−1922(4)	−58(6)	599(3)	20(2)
B(1)	−106(5)	5517(7)	7635(4)	22(3)
C(25)	−1645(4)	4485(5)	7897(3)	22(3)
C(24)	−2484(4)	4516(6)	8114(3)	20(3)
C(23)	−2794(4)	5618(6)	8330(3)	23(3)
C(22)	−2281(4)	6655(6)	8326(3)	27(3)
C(21)	−1453(4)	6605(6)	8111(3)	28(3)
C(20)	−1102(4)	5519(6)	7882(3)	17(2)
C(35)	1630(4)	5982(6)	8378(3)	31(3)
C(34)	2380(4)	5971(6)	9024(3)	33(3)
C(33)	2267(4)	5670(5)	9750(3)	27(3)
C(32)	1382(4)	5400(5)	9823(3)	25(3)
C(31)	639(4)	5419(5)	9171(3)	19(2)
C(30)	732(4)	5683(5)	8421(3)	20(3)
C(45)	−464(4)	6596(6)	6220(3)	25(3)
C(44)	−509(4)	7599(6)	5732(4)	32(3)
C(43)	−221(4)	8716(6)	6020(4)	34(3)
C(42)	151(5)	8842(7)	6820(4)	43(3)
C(41)	199(4)	7851(6)	7309(4)	31(3)
C(40)	−113(4)	6692(6)	7035(3)	21(2)
C(55)	885(4)	3575(5)	7387(3)	20(2)
C(54)	1020(4)	2530(6)	6992(3)	31(3)
C(53)	341(5)	2093(6)	6374(3)	30(3)
C(52)	−491(4)	2709(6)	6179(3)	25(3)
C(51)	−626(4)	3739(5)	6579(3)	22(2)
C(50)	53(4)	4245(5)	7196(3)	18(2)

[a]Equivalent isotropic U defined as one third of the trace of the orthogonalized U_{ij} tensor.

Preparation of compounds

$[Fe(L)](CF_3SO_3)_2\cdot C_4H_8O_2$, $L=bzo_2$-18S6

$FeC_2O_4\cdot2H_2O$ (179.9 mg, 1.0 mmol) and L (456.8 mg, 1.0 mmol) were refluxed with CF_3SO_3H (0.18 ml, 2.0 mmol) in 30 ml of dioxane for 1 h, in the course of which the product precipitated as a violet powder. It was filtered off, washed with dioxane, and dried *in vacuo*.

$[Fe(L)](CF_3SO_3)_2 \cdot C_4H_8O_2$: yield 818.2 mg (91%). *Anal.* Calc. for $C_{26}F_6FeH_{32}O_8S_8$: C, 34.74; H, 3.59%. Found: C, 34.48; H, 3.45%.

$[Fe(L)](CF_3SO_3)_2$

$FeC_2O_4 \cdot 2H_2O$ (179.9 mg, 1.0 mmol) and L (456.8 mg, 1.0 mmol) were refluxed with CF_3SO_3H (0.18 ml, 2.0 mmol) in 40 ml of $EtNO_2$ for 1 h. The reaction mixture was cooled to room temperature, filtered and cooled further down to −30 °C overnight. The precipitated violet microcrystals were filtered off, washed with THF, and dried *in vacuo*. Further product was obtained by evaporating the mother liquor to dryness and washing the residue with 50 ml of THF.

$[Fe(L)](CF_3SO_3)_2$: yield 537.6 mg (66%). *Anal.* Calc. for $C_{22}F_6FeH_{24}O_6S_8$: C, 32.59; H, 2.98%. Found: C, 32.70; H, 2.93%.

Violet crystals of $[Fe(L)](CF_3SO_3)_2$ were obtained by layering a solution of $[Fe(L)](CF_3SO_3)_2 \cdot C_4H_8O_2$ in $EtNO_2$ with Et_2O.

$[Co^{II}(L)](CF_3SO_3)_2 \cdot C_4H_8O_2$

$Co(CH_3COO)_2 \cdot 4H_2O$ (249.0 mg, 1.0 mmol) and L (456.8 mg, 1.0 mmol) were refluxed with CF_3SO_3H (0.18 ml, 2.0 mmol) in 35 ml of dioxane for 1 h. The resulting light brown precipitate was filtered off, washed with dioxane, and dried *in vacuo*.

$[Co^{II}(L)](CF_3SO_3)_2 \cdot C_4H_8O_2$: yield 847.8 mg (94%). *Anal.* Calc. for $C_{26}CoF_6H_{32}O_8S_8$: C, 34.62; H, 3.58; S, 28.44%. Found: C, 34.86; H, 3.53; S, 29.07%.

$[Co^{II}(L)][B(C_6H_5)_4]_2$

$CoCl_2$ (75.3 mg, 0.58 mmol) and L (263.7 mg, 0.58 mmol) were heated in 30 ml of n-BuOH giving a blue solution. Upon addition of $Na[B(C_6H_5)_4]$ (431.7 mg, 1.26 mmol), an ochre powder precipitated immediately. The suspension was heated to reflux for 1 h and after cooling to room temperature, the precipitate was filtered off, washed with MeOH, and dried *in vacuo*.

$[Co^{II}(L)][B(C_6H_5)_4]_2$: yield 610 mg (91%). *Anal.* Calc. for $B_2C_{68}CoH_{64}S_6$: C, 70.76; H, 5.59; S, 16.67%. Found: C, 70.68; H, 5.91; S, 16.88%.

$[Co^{III}(L)](CF_3SO_3)_3 \cdot C_4H_8O_2$

From $[Co^{II}(L)](CF_3SO_3)_2 \cdot C_4H_8O_2$. $[Co^{II}(L)](CF_3SO_3)_2 \cdot C_4H_8O_2$ (798.8 mg, 0.89 mmol) was suspended in 50 ml of dioxane, and CF_3SO_3H (0.1 ml, 1.14 mmol) and $NOBF_4$ (*c.* 110 mg, 0.94 mmol) were added, whereupon the colour of the reaction mixture changed from light brown to bright orange. After stirring at room temperature overnight, the precipitate was filtered off, washed with dioxane, and dried *in vacuo*. Yield 904.4 mg (97%).

From $[Co(C_5H_7O_2)_3]$, $C_5H_7O_2$ = acetylacetonate-(1−). $[Co(C_5H_7O_2)_3]$ (356.3 mg, 1.0 mmol), L (456.8 mg, 1.0 mmol) and CF_3SO_3H (0.53 ml, 6.0 mmol) were refluxed in 30 ml of dioxane for 1 h. The resulting orange–brown precipitate was filtered off, washed with dioxane and Et_2O, and resuspended in 60 ml of dioxane. After addition of CF_3SO_3H (0.18 ml, 2.0 mmol) and $NOBF_4$ (*c.* 120 mg, 1.03 mmol), the suspension was stirred overnight in the course of which its colour changed to a bright orange. The precipitate was filtered off, washed with dioxane, and dried *in vacuo*.

$[Co^{III}(L)](CF_3SO_3)_2 \cdot C_4H_8O_2$: yield 982.8 mg (94%). *Anal.* Calc. for $C_{27}CoF_9H_{32}O_{11}S_9$: C, 30.85; H, 3.07; S, 27.46%. Found: C, 31.15; H, 3.21; S, 27.09%.

Orange crystals of solvate free $[Co^{III}(L)](CF_3SO_3)_3$ were obtained by layering a solution of $[Co^{III}(L)](CF_3SO_3)_3 \cdot C_4H_8O_2$ in $EtNO_2$ with Et_2O. *Anal.* Calc. for $C_{23}CoF_9H_{24}O_9S_9$: C, 28.69; H, 2.51; S, 29.97%. Found: C, 28.96; H, 2.62, S, 30.44%.

$[Ni(L)](CF_3SO_3)_2 \cdot C_4H_8O_2$

$[Ni(C_5H_7O_2)_2]_3$ (256.9 mg, 0.33 mmol) and L (456.8 mg, 1.0 mmol) were refluxed with CF_3SO_3H (0.18 ml, 2.0 mmol) in 30 ml of dioxane for 30 min. The resulting light violet product was filtered off, washed with dioxane, and dried *in vacuo*.

$[Ni(L)](CF_3SO_3)_2 \cdot C_4H_8O_2$: yield 861.7 mg (96%). *Anal.* Calc. for $C_{26}F_6H_{32}NiO_8S_8$: C, 34.63; H, 3.58; S, 28.45%. Found: C, 34.66; H, 3.53; S, 28.40%.

Layering a solution of $[Ni(L)](CF_3SO_3)_2 \cdot C_4H_8O_2$ in $EtNO_2$ with a solution of $Na[B(C_6H_5)_4]$ in n-BuOH yielded brown–orange crystals of $[Ni(L)][B(C_6H_5)_4]_2$. *Anal.* Calc. for $B_2C_{68}H_{64}NiS_6$: C, 70.78; H, 5.59; S, 16.67%. Found: C, 71.04; H, 5.69; S, 16.95%.

$[Cu(L)](CF_3SO_3)_2 \cdot 0.5C_4H_8O_2$

$[Cu(CH_3COO)_2(H_2O)]_2$ (199.7 mg, 0.50 mmol) and L (456.8 mg, 1.0 mmol) were refluxed with CF_3SO_3H (0.18 ml, 2.0 mmol) in 35 ml of dioxane for 30 min. The resulting dark brown precipitate was filtered off, washed with Et_2O, and dried *in vacuo*.

$[Cu(L)](CF_3SO_3)_2 \cdot 0.5C_4H_8O_2$: yield 835.7 mg (97%). *Anal.* Calc. for $C_{24}CuF_6H_{28}O_7S_8$: C, 33.42; H, 3.27; S, 29.74%. Found: C, 33.56; H, 3.36; S, 29.78%.

Results and discussion

Synthesis and properties of $[M(L)]^{n+}$ (M = Fe, Ni, Cu: n = 2; M = Co: n = 2,3)

$[M(L)](CF_3SO_3)_2$ (M = Fe, Co, Ni, Cu) form in high yields, usually as voluminous powders, by reaction of metal oxalates, acetates or acetylacetonates with stoichiometric amounts of L in the presence of CF_3SO_3H in boiling dioxane (~101 °C) or $EtNO_2$ (~114 °C) according to eqn. (1).

$$MX + L + 2CF_3SO_3H \xrightarrow[-(X)H2]{\text{Dioxane or } EtNO_2/\text{reflux}} \left[\text{ 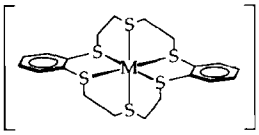 }\right](CF_3SO_3)_2 \quad (1)$$

$MX = FeC_2O_4$; $Co(CH_3CO_2)_2$; $Ni(C_5H_7O_2)_2$; $Cu(CH_3CO_2)_2$

When isolated from dioxane the complexes were obtained as dioxane solvates, whereas products isolated from $EtNO_2$ contained no solvent. The salts are stable towards air and well soluble in nitroalkanes, but insoluble in CH_2Cl_2, hexane, ethers and H_2O. Except $[Co^{II}(L)](CF_3SO_3)_2 \cdot C_4H_8O_2$ that is instantly oxidized to the Co(III) species, the salts are also well soluble in concentrated H_2SO_4 without decomposition. They are regained as sulfates from these solutions by dilution with Et_2O. All other common solvents cause decomposition in the course of which the ligand decoordinates from the metal centre. The rate of decomposition depends on the metal M and the solvent. While $[Cu(L)](CF_3SO_3)_2 \cdot 0.5C_4H_8O_2$ decomposes instantly upon addition of MeOH, it can be dissolved in CH_3CN yielding a dark brown solution which decolorizes only after several hours. In contrast, violet solutions of $[Ni(L)](CF_3SO_3)_2 \cdot C_4H_8O_2$ show greater stability in MeOH than in CH_3CN. The salts can be recrystallized from $EtNO_2$ layered with Et_2O. They are then usually obtained in thin needle-shaped crystals.

$[Fe(L)]^{2+}$, $[Ni(L)]^{2+}$ and $[Cu(L)]^{2+}$ are stable towards oxidation by $NOBF_4$ or $Pb(CH_3COO)_4$. $[Co^{II}(L)]^{2+}$, however, readily reacts with $NOBF_4$ in dioxane to give $[Co^{III}(L)]^{3+}$, according to eqn. (2).

$$[Co(bzo_2\text{-}18S6)](CF_3SO_3)_2 + NOBF_4 + CF_3SO_3H \xrightarrow{\text{Dioxane/20 °C}} [Co(bzo_2\text{-}18S6)](CF_3SO_3)_3 + HBF_4 + NO \quad (2)$$

$[Co^{III}(L)](CF_3SO_3)_3 \cdot C_4H_8O_2$ can also be obtained by direct synthesis from $[Co(C_5H_7O_2)_3]$, analogous to the reaction according to eqn. (1). It exhibits the same solubility as the $[M(L)]^{2+}$ salts, but a much larger stability towards decoordination of L in strong donor solvents. For instance, it can be dissolved in MeOH or CH_3CN without showing any decomposition. Metallic Zn or $LiBEt_3H$ reduce $[Co^{III}(L)]^{3+}$ to $[Co^{II}(L)]^{2+}$.

The $[M(L)]^{n+}$ cations are stable towards strong acids, e.g. H_2SO_4 or CF_3SO_3H. It was tested whether hydrides formed, but ^1H NMR spectra of these solutions did not show signals indicative of metal hydride formation. This holds also for $[Ru(L)]^{2+}$. Bases lead to rapid decomposition and products that could not yet be unambiguously identified. In this respect $[Fe(L)]^{2+}$, $[Co^{II}(L)]^{2+}$, $[Co^{III}(L)]^{3+}$, $[Ni(L)]^{2+}$ and $[Cu(L)]^{2+}$ contrast with $[Ru(L)]^{2+}$ that reacts with bases in a well defined way to give under S–C bond cleavage $[Ru('S_6'\text{-}CH{=}CH_2)]^+$ ('S_6'-$CH{=}CH_2^-$ = 2,3,11,12-dibenzo-1,4,7,10,13,16-hexathiaoctadeca-2,11,17-triene(1−)) [10].

X-ray structure determination of $[Ni(bzo_2\text{-}18S6)][B(C_6H_5)_4]_2$

The crystal structure of $[Ni(bzo_2\text{-}18S6)][B(C_6H_5)_4]_2$ consists of discrete cations and anions, the cations lying on crystallographic centres of symmetry. Figure 1 shows the molecular structure of the $[Ni(bzo_2\text{-}18S6)]^{2+}$ cation; Table 3 lists selected distances and angles.

In the centrosymmetric $[Ni(L)]^{2+}$ the nickel is surrounded pseudooctahedrally by the six sulfur atoms of L. The Ni–S bond lengths differ only slightly within the range of 237.5–240.1 pm (average 238.9 pm). The *cis*-S–Ni–S bond angles are 90 ± 2.3° (range 87.7–92.3°) while the *trans*-S–Ni–S bond angles are required by the inversion symmetry to be 180°. With regard to distances and angles $[Ni(L)]^{2+}$ compares well with the cation of $[Ni(18S6)](picrate)_2$ [11]. As all Ni–S bonds are shorter than the sum of the covalent radii of Ni(II) (139 pm) and thioether sulfur (105 pm) [12, 13], $[Ni(L)]^{2+}$ also reveals a ligand compression effect [14].

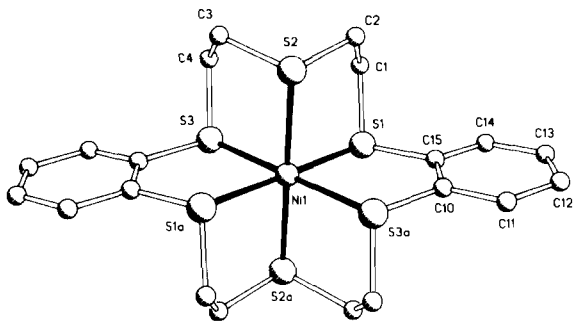

Fig. 1. Molecular structure of $[Ni(bzo_2\text{-}18S6)]^{2+}$ (H atoms omitted).

TABLE 3. Selected distances (pm) and angles (°) of $[Ni(bzo_2\text{-}18S6)]^{2+}$ in $[Ni(bzo_2\text{-}18S6)][B(C_6H_5)_4]_2$

Ni(1)–S(1)	239.1(2)	S(1)–Ni(1)–S(2)	88.9(1)
Ni(1)–S(2)	237.5(2)	S(1)–Ni(1)–S(3)	92.3(1)
Ni(1)–S(3)	240.1(2)	S(2)–Ni(1)–S(3)	89.1(1)
S(1)–C(1)	180.9(5)	S(2)–Ni(1)–S(1A)	91.1(1)
S(1)–C(15)	179.1(7)	S(3)–Ni(1)–S(1A)	87.7(1)
S(2)–C(2)	181.2(6)	S(3)–Ni(1)–S(2A)	90.0(1)
S(2)–C(3)	181.5(6)	Ni(1)–S(1)–C(1)	101.2(2)
S(3)–C(4)	182.5(5)	Ni(1)–S(1)–C(15)	103.6(2)
S(3)–C(10A)	179.8(7)	C(1)–S(1)–C(15)	100.2(3)
C(1)–C(2)	152.7(7)	Ni(1)–S(2)–C(2)	102.6(2)
C(3)–C(4)	151.6(8)	Ni(1)–S(2)–C(3)	101.4(2)
C(15)–C(14)	138.6(9)	C(2)–S(2)–C(3)	105.0(3)
C(15)–C(10)	137.8(10)	Ni(1)–S(3)–C(4)	102.3(2)
C(14)–C(13)	138.6(10)	Ni(1)–S(3)–C(10A)	102.9(2)
C(13)–C(12)	137.1(11)	C(4)–S(3)–C(10A)	100.4(3)
C(12)–C(11)	138.4(10)		
C(11)–C(10)	139.6(9)		

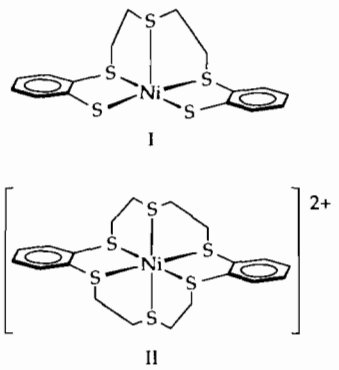

I II

Fig. 2. Structures of $[Ni('S_5')]$ (I) and $[Ni(L)]^{2+}$ (II).

The slightly distorted NiS_6 core is observed in all Ni–hexakis-thioether complexes that were hitherto structurally characterized [11, 15–17]. The distances in $[Ni(L)]^{2+}$ between the metal and the aromatic thioether atoms are almost identical (240.1; 239.1 pm), whereas the bond lengths from Ni to the alkylic thioethers are shorter (237.5 pm).

Structure and properties of the $[Ni(bzo_2\text{-}18S6)]^{2+}$ ion are of interest with regard to the closely related $[Ni('S_5')]$ ($'S_5'^{2-}$ = 2,2′-bis(2-mercaptophenylthio)-diethylsulfide(2−)) [18]. $[Ni('S_5')]$ as well as $[Ni(L)]^{2+}$ contain Ni(II) and differ formally only in one $S(C_2H_4-)_2$ fragment as shown in Fig. 2. The Ni centre in $[Ni(L)]^{2+}$, however, is surrounded only by thioether S atoms, whereas the Ni centre in the square pyramidal $[Ni('S_5')]$ is ligated by three thioether and two thiolate donors. This leads to remarkably different properties of the two species that are compared in Table 4.

$[Ni('S_5')]$ and $[Ni(L)]^{2+}$ are electronically different, the former being diamagnetic, the latter paramagnetic having two antibonding electrons. This causes different Ni–S bond lengths. $[Ni('S_5')]$ has four short and one very long Ni–S bonds; in $[Ni(L)]^{2+}$ all six Ni–S bonds are virtually equal and *c.* 20 pm longer than the average bond length in the square planar NiS_4 array of $[Ni('S_5')]$. These differences might also be responsible for the stability of $[Ni('S_5')]$ towards solvolysis, in contrast to $[Ni(L)]^{2+}$ that is already decomposed by MeOH.

TABLE 4. Properties of $[Ni('S_5')]$ and $[Ni(L)]^{2+}$

	$[Ni('S_5')]$	$(Ni(L)]^{2+}$
S-donors	3 thioethers +2 thiolates	6 thioethers
Coordination	[4+1]	[6]
Ni–S distances (pm)	217.6(3), 219.7(4) 220.4(3), 222.3(3) 274.7(4)	2×237.5(2) 2×239.1(2) 2×240.1(2)
Magnetism	diamagnetic	paramagnetic

The differences between $[Ni('S_5')]$ and $[Ni(L)]^{2+}$ are certainly due also to the different ligand properties of thiolate and thioether S donors. Thiolate S atoms possess π-donor and thioether S atoms rather π-acceptor properties. Consequently in $[Ni('S_5')]$ π-donor and π-acceptor bonds mutually strengthen Ni–S bonds according to Scheme 1. In $[Ni(L)]^{2+}$, however, only π-acceptor bonds are possible.

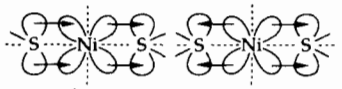

π-donor + π-acceptor in $[Ni('S_5')]$ | π-acceptor only in $[Ni(L)]^{2+}$

Scheme 1

Spectra and electrochemistry of $[M(L)]^{n+}$

IR spectra of $[M(L)]^{n+}$ salts in the range from 4000–400 cm^{-1} show the typical ligand and anion bands, but yield no information with regard to structure. In the mass spectra, $\{[Co^{II}(L)](CF_3SO_3)\}^+$ (m/e = 664), $[Ni(L)]^{2+}$ (m/e = 257) and $\{[Cu(L)](CF_3SO_3)\}^+$ (m/e = 668) are detectable. The FD mass spectrum of $[Fe(L)](CF_3SO_3)_2$ exhibits the ligand signal only at m/e = 456, whereas $[Co^{III}(L)](CF_3SO_3)_3 \cdot C_4H_8O_2$ shows only decomposition products.

$[Co^{II}(L)](CF_3SO_3)_2 \cdot C_4H_8O_2$, $[Ni(L)](CF_3SO_3)_2 \cdot C_4H_8O_2$ and $[Cu(L)](CF_3SO_3)_2 \cdot 0.5C_4H_8O_2$ are paramagnetic with μ_{eff} values of 2.12, 2.82 and 1.64 BM, respectively. The magnetism of $[Ni(L)](CF_3SO_3)_2 \cdot C_4H_8O_2$ and $[Cu(L)](CF_3SO_3)_2 \cdot 0.5C_4H_8O_2$ corresponds well with the expected spin-only magnetic moments of octahedral Ni(II) and Cu(II) complexes. $[Co^{II}(L)]^{2+}$ represents one of the rare examples of low spin six coordinate Co^{2+} com-

plexes. The μ_{eff} of $[Co^{II}(L)](CF_3SO_3)_2 \cdot C_4H_8O_2$ indicates spin orbit coupling.

In the ^1H NMR spectra of paramagnetic $[Co^{II}(L)](CF_3SO_3)_2 \cdot C_4H_8O_2$, $[Ni(L)](CF_3SO_3)_2 \cdot C_4H_8O_2$ and $[Cu(L)](CF_3SO_3)_2 \cdot 0.5C_4H_8O_2$ only the dioxane signal could be observed. $[Fe(L)](CF_3SO_3)_2 \cdot C_4H_8O_2$ and $[Co^{III}(L)](CF_3SO_3)_3 \cdot C_4H_8O_2$ in CD_3NO_2 yield well resolved ^1H NMR spectra, the first one showing two multiplets for the aromatic protons at 8.18 and 7.80 ppm and three multiplets for the aliphatic protons at 3.53, 3.06 and 1.93 ppm. The dioxane singlet appears at 3.58 ppm. With the exception of the dioxane signal, the spectrum resembles that of $[Ru(L)]^{2+}$ salts showing the same splitting patterns with only slightly different chemical shifts. Apparently, also the Fe(II) centre in $[Fe(L)]^{2+}$ is octahedrally coordinated by the six sulfur donors of the ligand. The ^{13}C NMR spectrum of $[Fe(L)](CF_3SO_3)_2 \cdot C_4H_8O_2$ further suggests a structure analogous to that of $[Ru(L)]^{2+}$ and $[Ni(L)]^{2+}$. The number of signals requires the $[Fe(L)]^{2+}$ cation to possess a mirror plane and to exhibit the *meso*-configuration as observed for the ruthenium and nickel complexes by X-ray crystallography.

The dioxane and aliphatic C atom signals of $[Fe(L)](CF_3SO_3)_2 \cdot C_4H_8O_2$ are broadened. This possibly indicates interaction of the alkylic thioether and the dioxane molecules due to reversible decoordination of apical thioethers and coordination of dioxane. In $[Fe(L)](CF_3SO_3)_2$ having no dioxane solvate, the respective alkylic thioether C atoms give rise to sharp ^{13}C signals.

The ^1H NMR spectrum of $[Co^{III}(L)](CF_3SO_3)_3 \cdot C_4H_8O_2$ exhibits the aromatic protons at 8.30 and 8.04 ppm and the aliphatic ones at 4.23, 4.00 and 3.09 ppm. The dioxane signal is located at 3.60 ppm. The ^{13}C NMR spectrum shows three signals for the aromatic, two signals for the aliphatic and one for the C atoms of the dioxane. The quadruplet of the CF_3 group appears at 122.5 ppm. As described previously, the dioxane and aliphatic C atom signals are also broadened. Table 5 lists ^1H and ^{13}C NMR data.

The UV–Vis spectra of $[M(L)]^{2+}$ show bands in the range from 250–800 nm. The occurring bands cannot be assigned unambiguously, as they are partially obscured by bands of L showing π–π^* transitions in the range from 220–330 nm, so that determination of the ligand field strength of L is not possible. UV–Vis spectroscopic and magnetic data are summarized in Table 6.

Cyclovoltammetric properties of $[M(L)](CF_3SO_3)_n \cdot mC_4H_8O_2$ show similarities as well as remarkable differences with respect to corresponding 18S6 (= 1,4,7,10,13,16-hexathiacyclooctadecane) and 9S3 (= 1,4,7-trithiacyclononane) compounds. $[Fe(L)](CF_3SO_3)_2 \cdot C_4H_8O_2$ is redox inert in the range from +2.0 to −1.7 V. The corresponding 9S3 compound $[Fe(9S3)_2]^+$, however, is reversibly oxidized at +0.98 V versus ferrocene [19].

$[Co^{II}(L)](CF_3SO_3)_2 \cdot C_4H_8O_2$ in CH_3CN shows two reversible redox waves at +0.78 and −0.15 V due to the $[Co(L)]^{2+/3+}$ and $[Co(L)]^{2+/+}$ couples, respectively. In addition to these two waves an irreversible wave at +0.47 V can be observed. It does not occur when the cyclovoltammogram is run in $MeNO_2$, which means that it arises from decomposition products of $[Co(L)]^{2+}$ which are formed in CH_3CN. In $MeNO_2$, however, the two waves at +0.78 and −0.15 V become quasireversible. Figure 3 shows the cyclovoltammogram of $[Co(L)]^{2+}$ in CH_3CN. The behaviour of $[Co(L)]^{2+}$ contrasts with the redox behaviour of $[Co^{II}(18S6)](picrate)_2$, but resembles that of $[Co^{II}(9S3)_2]^{2+}$. $[Co^{II}(18S6)](picrate)_2$ shows one reversible wave at +0.844 V for the $[Co(18S6)]^{2+/3+}$ couple and one irreversible reduction wave at −0.16 V [20]. $[Co^{II}(9S3)_2]^{2+}$ also shows two reversible waves at +0.57 and −0.29 V and one additional irreversible reduction wave at −1.0 V [21].

$[Ni(L)](CF_3SO_3)_2 \cdot C_4H_8O_2$ in CH_3NO_2 is redox inert in the range from 0 to +2.0 V, but yields one irreversible reduction wave at −0.56 V. $[Ni(18S6)]^{2+}$ has not been investigated electrochemically. The corresponding 9S3 complex $[Ni(9S3)_2]^{2+}$ yields only one quasireversible oxidation wave at +0.97 V versus ferrocene [19].

$[Cu(L)](CF_3SO_3)_2 \cdot 0.5C_4H_8O_2$ is quasireversibly oxidized at +0.92 V. An irreversible reduction wave occurs at −0.66 V. Thus we assign the observed waves at +0.92 and −0.66 V to the $[Cu(L)]^{2+/3+}$ and $[Cu(L)]^{2+/+}$ couples, respectively. $[Cu(L)]^+$ undergoes rapid decomposition, the products of which give rise to the irreversible wave at −0.22 V. These results contrast remarkably with the redox behavior of $[Cu(18S6)]^{2+}$. It is described by Hartman and Cooper to show only one reversible wave at +0.96 V, which is assigned to a $[Cu(18S6)]^{2+/+}$ couple [22]. Figure 4 shows the cyclic voltammogram of $[Cu(L)](CF_3SO_3)_2 \cdot 0.5C_4H_8O_2$ in CH_3CN. Table 7 lists the electrochemical data.

The inertness of the Fe and Ni complexes towards oxidation might be a consequence of metal thioether bonding, structure and electron configuration. In the case of iron six π-accepting thioethers form π-bonds with occupied d-orbitals and the Fe electrons become strongly bonding. Further, removal of one of the electrons is expected to lead to Fe–S bond elongation. This can be deduced from the observation of Schröder and co-workers with the $[Fe(9S3)_2]^{2+/3+}$ complexes. Whereas in $[Fe(9S3)_2]^{2+}$ all six Fe–S bonds are equal,

TABLE 5. NMR spectroscopic data of $[M(L)](CF_3SO_3)_n$

Compound	^1H NMR, δ (ppm)	^{13}C NMR, δ (ppm)
$[Fe(L)(CF_3SO_3)_2 \cdot C_4H_8O_2$[a]	8.18, 7.80 (m, C_6H_4) 3.53, 3.06, 1.93 (m, C_2H_4) 3.58 (s, Dioxane)	136.9, 134.5, 133.4 (C_6H_4) 122.5 (CF_3) 48.9, 38.7 (C_2H_4) 68.1 (Dioxane)
$[Co^{III}(L)](CF_3SO_3)_3 \cdot C_4H_8O_2$[a]	8.30, 8.04 (m, C_6H_4) 4.23, 4.00, 3.09 (m, C_2H_4) 3.60 (s, Dioxane)	136.9, 134.4, 134.3 (C_6H_4) 122.5 (CF_3) 44.0, 55.0 (C_2H_4) 68.1 (Dioxane)

[a] In CD_3NO_2.

TABLE 6. UV–Vis spectroscopic and magnetic data of $[M(L)]^{n+}$

Ion	Colour	λ_{max} (nm)	ϵ (M^{-1} cm^{-1})	μ_{eff} (BM)
$[Fe(L)]^{2+}$[a]	purple	260.5	8045	
		274.0	4855	
		391.0	69	
		529.0	42	
$[Co^{II}(L)]^{2+}$[b]	brown	371.0	4093	2.12
$[Co^{III}(L)]^{3+}$[a]	orange	311.5	15150	
		370.0	3920	
$[Ni(L)]^{2+}$[a]	pale violet	274.5	5380	2.82
		314.5	6950	
		505.0	30	
		783.0	26	
$[Cu(L)]^{2+}$[a]	dark brown	268.0	3360	1.64
		351.5	2060	
		441.5	4820	

[a] In conc. H_2SO_4. [b] In CH_3NO_2, other expected absorptions are obscured by the solvent.

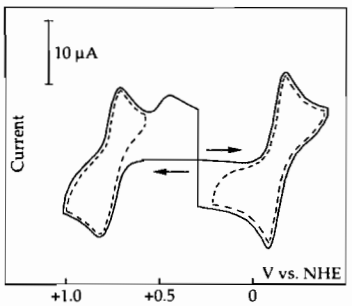

Fig. 3. Cyclic voltammogram of $[Co(L)](CF_3SO_3)_2 \cdot C_4H_8O_2$ in CH_3CN (10^{-3} M, 0.1 M $TBAClO_4$, 100 mV s^{-1}).

in $[Fe(9S3)_2]^{3+}$ two Fe–S bonds have become longer [23]. In $[Fe(L)]^{2+}$, the rigidity of L obviously hinders such an elongation of two bonds.

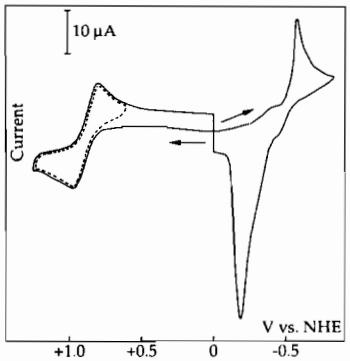

Fig. 4. Cyclic voltammogram of $[Cu(L)](CF_3SO_3)_2 \cdot 0.5C_4H_8O_2$ in CH_3CN (10^{-3} M, 0.1 M $TBAClO_4$, 20 mV s^{-1}).

TABLE 7. Electrochemical data of $[M(L)]^{n+}$

Couple	E^0 (V)	ΔE_p (V)	Reversibility
$[Fe(L)]^{2+/3+}$			
$[Co(L)]^{2+/3+}$	+0.78	0.066	rev.
$[Co(L)]^{2+/+}$	−0.15	0.067	rev.
$[Ni(L)]^{2+/+}$	−0.56		irrev.
$[Cu(L)]^{2+/3+}$	+0.92	0.18	quasirev.
$[Cu(L)]^{2+/+}$	−0.66		irrev.

In the case of nickel easy oxidation could be expected, because two electrons are antibonding. Oxidation to a d^6 Ni(IV) complex, however, would require a drastic shortening of the Ni–S bonds from about 240 to about 220 pm and less. Again the rigid L frame is apparently not flexible enough to allow such a shortening and, consequently, $[Ni(L)]^{2+}$ becomes stable towards oxidation.

Electronic and structural effects may also explain the redox behaviour of the Co and Cu complexes. $[Co(L)]^{2+}$ is expected to exhibit Jahn–Teller dis-

tortion that should favour the removal of the antibonding odd electron and in d^6 $[Co(L)]^{3+}$ all six Co–S bonds should have identical lengths.

The same may hold for $[Cu(L)]^{2+/3+}$. Removal of one electron of the Cu(II) d^9 system leads to a d^8 system that should be less distorted.

The observations reflect the cooperation of the structural influences of the bzo_2-18S6 ligand and the electronic configuration of the coordinated metal centres. They show that structural rigidity can be a determining factor for redox behaviour.

Conclusions

Coordination of bzo_2-18S6 to Fe(II), Co(II), Ni(II) and Cu(II) leads to the homoleptic crown thioether complexes $[Fe(bzo_2\text{-}18S6)]^{2+}$, $[Co^{II}(bzo_2\text{-}18S6)]^{2+}$, $[Ni(bzo_2\text{-}18S6)]^{2+}$ and $[Cu(bzo_2\text{-}18S6)]^{2+}$, respectively. Other 3d metal ions, e.g. Cr^{3+}, Mn^{2+}, Zn^{2+}, showed no tendency to form complexes with bzo_2-18S6. The isolated complexes prove that, despite its unfavourable preorganization with only exodentate thioethers in the free state [2], bzo_2-18S6 like 18S6, is able to form octahedral complexes.

The results further show that complexes with metal sulfur cores can be redox active as well as redox inactive. In the case of homoleptic thioether complexes redox activity depends on the electronic configuration of the metal as well as on the geometry of the ligand. The rigidity of bzo_2-18S6 apparently favours oxidation of $[Co(L)]^{2+}$, but prevents it in the case of $[Fe(L)]^{2+}$ and $[Ni(L)]^{2+}$. The general assumption that metal sulfur complexes ought to be highly redox active is apparently a prejudice and not justified. They can be redox active as well as highly inert.

In conclusion the results indicate that thioether coordination alone may not be responsible for the redox activity of metal sulfur redox enzymes, e.g. blue copper proteins. In these proteins, the metals are also coordinated by thiolates [24], and redox activity may well be due to the simultaneous presence of metal thioether and metal thiolato bonds. The pseudotetrahedral coordination of Cu in the blue copper proteins is also an example of the structural influence on redox properties as was observed in this work with $[M(L)]^{n+}$ complexes.

Supplementary material

Further details of X-ray crystal structure analysis have been deposited and can be obtained from the Fachinformationszentrum Energie, Physik, Mathematik, D-7514 Eggenstein-Leopoldshafen 2 by citing the deposition no. CSD 320256, the authors and reference.

Acknowledgements

These investigations were supported by the Deutsche Forschungsgemeinschaaft and the Fonds der Chemischen Industrie. We gratefully acknowledge this support.

References

1 D. Sellmann, S. Fünfgelder and F. Knoch, *Z. Naturforsch.*, in press.
2 (a) D. Sellmann, P. Frank and F. Knoch, *J. Organomet. Chem., 339* (1988) 345; (b) D. Sellmann and P. Frank, *Angew. Chem., 98* (1986) 1115; *Angew. Chem., Int. Ed. Engl., 25* (1986) 1107.
3 C. J. Pedersen, *J. Am. Chem. Soc., 85* (1963) 553.
4 (a) A. Müller and B. Krebs (eds.), *Sulfur, its Significance for Chemistry, for Geo, Bio and Cosmosphere and Technology,* Elsevier, Amsterdam, 1984; (b) Th. G. Spiro (ed.), *Iron Sulfur Proteins,* Wiley, New York, 1982.
5 (a) S. R. Cooper, *Acc. Chem. Res., 21* (1988) 141; (b) S. R. Cooper and S. C. Rawle, *Struct. Bonding (Berlin) 72* (1990) 1.
6 A. J. Blake and M. Schröder, *Adv. Inorg. Chem., 35* (1990) 1.
7 D. Sellmann, H.-P. Neuner, R. Eberlein, M. Moll and F. Knoch, *Inorg. Chim. Acta, 175* (1990) 231.
8 B. E. Bryant and W. C. Frenelius, *Inorg. Synth., 5* (1957) 188.
9 H. W. Watson, Jr. and Chi-Tsun Lin, *Inorg. Chem., 5* (1966) 1074.
10 D. Sellmann, H.-P. Neuner, M. Moll and F. Knoch, *Z. Naturforsch., Teil B, 46* (1991) 303.
11 E. J. Hintsa, J. R. Hartman and S. R. Cooper, *J. Am. Chem. Soc., 105* (1983) 3738.
12 S. G. Murray and F. R. Hartley, *Chem. Rev., 81* (1981) 365.
13 L. A. Drummond, K. Henrick, M. J. L. Kanagasundaram, L. F. Lindoy, M. McPartin and P. A. Tasker, *Inorg. Chem., 21* (1982) 3923.
14 (a) Y. Hung, L. Y. Martin, S. C. Jackels, A. M. Tait and D. H. Busch, *J. Am. Chem. Soc., 99* (1977) 4029; (b) L. Y. Martin, L. J. De Hayes, L. J. Zompa and D. H. Busch, *J. Am. Chem. Soc., 96* (1974) 4046.
15 W. N. Setzer, C. A. Ogle, G. S. Wilson and R. S. Glass, *Inorg. Chem., 22* (1983) 266.
16 S. C. Rawle, J. R. Hartman, D. J. Watkin and S. R. Cooper, *J. Chem. Soc., Chem. Comm.,* (1986) 1083.
17 S. R. Cooper, S. C. Rawle, J. R. Hartman, E. J. Hintsa and G. A. Adams, *Inorg. Chem., 27* (1988) 1209.
18 D. Sellmann, S. Fünfgelder, G. Pöhlmann, F. Knoch and M. Moll, *Inorg. Chem., 29* (1990) 4772.

19 K. Wieghardt, H.-J. Küppers and J. Weiss, *Inorg. Chem., 24* (1985) 3067.
20 J. R. Hartman, E. J. Hintsa and S. R. Cooper, *J. Am. Chem. Soc., 108* (1986) 1208.
21 G. S. Wilson, D. D. Swanson and R. S. Glass, *Inorg. Chem., 25* (1986) 3827.
22 J. R. Hartman and S. R. Cooper, *J. Am. Chem. Soc., 108* (1986) 1202.
23 A. J. Blake, A. J. Holder, T. I. Hyde and M. Schröder, *J. Chem. Soc., Chem. Commun.,* (1986) 1433.
24 D. R. McMillan, *J. Chem. Educ., 62* (1985) 997.